HORIE, H., HUSEBYE, S., KATO, M., MEYERS, E. A., MUTO, Y., SUZUKI, I., TOKII, T. & ZINGARO, R. A. (1986). *Acta Chem. Scand. Ser. A*, **40**, 579–589.
HORIE, H., TOKII, T., MUTO, Y., STEWARD, O. W., CHANG, S.-C., SUZUKI, I., UEKUSA, H., OHBA, S., HUSEBYE, S. & KATO, M. (1992). In preparation.
JOHNSON, C. K. (1971). *ORTEP*II. Report ORNL-3794. Oak Ridge National Laboratory, Tennessee, USA.
KAHN, O. (1985). *Magneto-Structural Correlations in Exchange Coupled Systems*, edited by R. D. WILLET, D. GATTESCHI & O. KAHN, pp. 37–56. Dordrecht: D. Reidel.
KATO, M. & MUTO, Y. (1988). *Coord. Chem. Rev.* **92**, 45–83.
KAWATA, T., UEKUSA, H., OHBA, S., FURUKAWA, T., TOKII, T., MUTO, Y. & KATO, M. (1992). *Acta Cryst.* B**48**, 253–261.
MORELAND, J. A. & DOEDENS, J. R. (1975). *J. Am. Chem. Soc.* **97**, 508–513.
MORELAND, J. A. & DOEDENS, J. R. (1978). *Inorg. Chem.* **17**, 674–677.
MUTO, Y., NAKASHIMA, M., TOKII, T., KATO, M. & SUZUKI, I. (1987). *Bull. Chem. Soc. Jpn*, **60**, 2849–2853.
NAKASHIMA, M., MIKURIYA, M. & MUTO, Y. (1985). *Bull. Chem. Soc. Jpn*, **58**, 968–973.
PORTER, L. C., DICKMAN, M. H. & DOEDENS, R. J. (1986). *Inorg. Chem.* **25**, 678–684.
SAKURAI, T. & KOBAYASHI, K. (1979). *Rikagaku Kenkyusho Hokoku*, **55**, 69–77.
STEWARD, O. W., DZIEDZIC, J. E., JOHNSON, J. S. & FROHLIGER, J. O. (1971). *J. Org. Chem.* **36**, 3480–3484.
STEWARD, O. W., KATO, M., CHANG, S. C., SAX, M., CHANG, C. H., JURY, C. F., MUTO, Y., TOKII, T., TAURA, T., PLETCHER, J. & YOO, C. S. (1991). *Bull. Chem. Soc. Jpn*, **63**, 3046–3058.
STEWARD, O. W., MCAFEE, R. C., CHANG, S. C., PISKOR, S. R., SCHREIBER, W. J., JURY, C. F., TAYLOR, C. E., PLETCHER, J. F. & CHEN, C. S. (1986). *Inorg. Chem.* **25**, 771–777.
UEKUSA, H., OHBA, S., SAITO, Y., KATO, M., STEWARD, O. W., TOKII, T. & MUTO, Y. (1990). *Acta Cryst.* C**46**, 1805–1812.
YAMANAKA, M., UEKUSA, H., OHBA, S., SAITO, Y., IWATA, S., KATO, M., TOKII, T., MUTO, Y. & STEWARD, O. W. (1991). *Acta Cryst.* B**47**, 344–455.

Acta Cryst. (1992). B**48**, 667–672

Electron-Density Distribution in Crystals of *lel*$_3$-[*M*(chxn)$_3$](NO$_3$)$_3$.3H$_2$O (*M* = Cr, Rh; chxn = *trans*-1,2-diaminocyclohexane) at 120 K

BY MITSUO MOROOKA AND SHIGERU OHBA*

Department of Chemistry, Faculty of Science and Technology, Keio University, Hiyoshi 3-14-1, *Kohoku-ku, Yokohama* 223, *Japan*

AND HIROSHI MIYAMAE

Department of Chemistry, Faculty of Science, Josai University, Keyakidai 1-1, *Sakado-shi, Saitama* 350-02, *Japan*

(*Received* 23 *January* 1992; *accepted* 13 *April* 1992)

Abstract

The electron-density distributions in non-centrosymmetric crystals containing Cr^{III} or Rh^{III} complexes with *trans*-1,2-diaminocyclohexane (chxn) as a bidentate ligand have been investigated by the multipole expansion method based on X-ray intensities collected at 120 K with Mo $K\alpha$ radiation (λ = 0.71073 Å). Crystals of the Cr^{III} and Rh^{III} complexes are isomorphous and hexagonal $P6_3$, $Z = 2$. (I): $\Delta(\lambda\lambda\lambda)$-tris(*trans*-1,2-diaminocyclohexane)-chromium(III) nitrate trihydrate, [Cr(C$_6$H$_{14}$N$_2$)$_3$](NO$_3$)$_3$.3H$_2$O, M_r = 634.6, $F(000)$ = 678, a = 13.029 (2), c = 10.040 (2) Å, V = 1476.0 (5) Å^3, D_x = 1.43 Mg m^{-3}, μ = 0.444 mm^{-1}, R = 0.041 for 3914 reflections. (II): $\Delta(\lambda\lambda\lambda)$-tris(*trans*-1,2-diaminocyclohexane)rhodium(III) nitrate trihydrate, [Rh(C$_6$H$_{14}$N$_2$)$_3$](NO$_3$)$_3$.3H$_2$O, M_r = 685.5, $F(000)$ = 720, a = 13.101 (2), c = 9.984 (2) Å, V = 1484.0 (5) Å^3, D_x = 1.53 Mg m^{-3}, μ = 0.632 mm^{-1}, R = 0.028 for 4602 reflections. The electron populations of the *d* orbitals of Cr^{III} and Rh^{III} atoms in a chemical D_3 ligand field were estimated and compared with those of the *lel*$_3$-Co^{III} complex. Phase improvement is necessary even when the valence-/core-electron ratio becomes smaller, because the phases based on the independent atom model are poor for one of the hexadecapole densities of the metal atoms in the title crystals.

Introduction

It is well-known that deformation densities of non-centrosymmetric structures suffer from phase error and the features are much smeared if the phase angle of F_o is estimated based on the spherical independent atom model (IAM). This inadequacy can be removed by the aspherical-atom model (Hirshfeld, 1971). In a previous paper (Morooka, Ohba, Saito & Miyamae,

* To whom correspondence should be addressed.

0108-7681/92/050667-06$06.00

Table 1. *Experimental information for (A) conventional and (B) multipole refinements*

	Cr		Rh	
	A	*B*	*A*	*B*
No. of reflections	3914	3914	4602	4602
No. of parameters	184	319	184	319
$R(F)$	0.048	0.041	0.031	0.028
$wR(F)$	0.037	0.028	0.030	0.025
S	1.25	0.97	1.17	0.99

1991), phase improvement for lel_3- and ob_3-$[Co(chxn)_3](NO_3)_3.3H_2O$ crystals was carried out by the multipole expansion method. Unexpectedly, it was found that the effect of phase improvement on the deformation densities around the Co atoms is anisotropic. This peculiarity was rationalized by considering the contributions of two hexadecapole densities, ρ_{40} and ρ_{43-}, to the structure factors. In the present study, lel_3-$[M(chxn)_3](NO_3)_3.3H_2O$ (M = Cr, Rh) crystals have been examined in order to investigate the necessity of phase improvement for metal atoms with a lower valence-/core-electron ratio than for the Co atom. The Cr^{III}, Co^{III} and Rh^{III} crystals are isostructural, and the metal atoms lie on a crystallographic threefold axis. Crystal structure analysis and a preliminary study of the electron-density distribution in lel_3- and ob_3-Rh^{III} complexes has already been carried out at room temperature (Miyamae, Sato & Saito, 1977; Miyamae, 1977).

Preparation, separation and characterization of the $[Cr(chxn)_3]^{3+}$ (Harnung & Laier, 1978) and $[Rh(chxn)_3]^{3+}$ (Galsbøl, Steenbøl & Sørensen, 1972) complexes have been reported as well as those of the Co^{III} complexes (Harnung, Sørensen, Creaser, Maegaard, Pfenninger & Schäffer, 1976), and the Ir^{III} systems (Galsbøl, 1978).

Experimental

Data collection

Crystals of $\Delta(\lambda\lambda\lambda)$-$[M(R,R\text{-chxn})_3](NO_3)_3.3H_2O$ (M = Cr, Rh) were kindly supplied by Dr F. Galsbøl of the H. C. Ørsted Institute, University of Copenhagen.

(I): An orange hexagonal prismatic crystal of the Cr complex was shaped into a sphere of 0.56 (1) mm in diameter and mounted on a Rigaku AFC-5 four-circle diffractometer. Data collection was carried out with graphite-monochromatized Mo $K\alpha$ radiation at 120 (2) K by using a nitrogen-gas-flow cooling unit. θ–2θ scan technique was adopted with scan speed 6° min^{-1} in θ and scan width $(1.3 + 0.36\tan\theta)°$. Range of indices, $-18 \le (h,k) \le 18$, $0 \le l \le 14$ ($4 < 2\theta \le 60°$); $0 \le (h,k) \le 28$, $0 \le l \le 21$ ($60 < 2\theta \le 100°$). Five standard reflections showed no significant variation, $0.995 < |F_o|/|F_o|_{initial} < 1.009$. 13162 reflections were measured, 11011 reflections were observed with $|F_o| > 3\sigma(|F_o|)$, and 3914 unique reflections were obtained ($R_{int} = 0.017$). Lattice constants were determined based on 25 2θ values ($22 < 2\theta < 32°$). Analytical corrections for absorption were made with $\mu r = 0.124$ assuming a spherical crystal shape (transmission factors $0.831 < A < 0.834$).

Table 2. *Positional parameters ($\times 10^4$) and equivalent isotropic temperature factors*

$B_{eq} = (8\pi^2/3)\sum_i\sum_j U_{ij}a_i^*a_j^*\mathbf{a}_i.\mathbf{a}_j$.

	x	y	z	B_{eq}(Å^2 × 10)
Compound (I)				
Cr	3333	6667	0	7 (1)
N(1)	2193 (1)	5228 (1)	−1196 (1)	9 (1)
N(2)	3297 (1)	5354 (1)	1196 (1)	9 (1)
C(1)	2388 (1)	4228 (1)	−824 (1)	11 (1)
C(2)	2367 (1)	4173 (1)	690 (1)	11 (1)
C(3)	2529 (1)	3166 (1)	1204 (2)	21 (1)
C(4)	1604 (2)	1981 (1)	592 (3)	30 (1)
C(5)	1673 (2)	2049 (1)	−947 (2)	26 (1)
C(6)	1480 (1)	3051 (1)	−1435 (2)	16 (1)
N(3)	5945 (1)	5129 (1)	946 (1)	13 (1)
O(1)	5526 (1)	5367 (1)	1936 (1)	25 (1)
O(2)	5655 (1)	5264 (1)	−215 (1)	18 (1)
O(3)	6631 (1)	4723 (1)	1100 (1)	21 (1)
O(*W*)	7970 (1)	5066 (1)	−1321 (2)	19 (1)
Compound (II)				
Rh	3333	6667	0	8 (1)
N(1)	2168 (1)	5245 (1)	−1179 (1)	11 (1)
N(2)	3339 (1)	5377 (1)	1188 (1)	11 (1)
C(1)	2370 (2)	4251 (1)	−825 (2)	12 (1)
C(2)	2394 (2)	4205 (2)	694 (2)	14 (1)
C(3)	2550 (2)	3197 (1)	1195 (2)	24 (1)
C(4)	1618 (3)	2021 (2)	595 (4)	33 (1)
C(5)	1635 (3)	2080 (2)	−939 (3)	31 (1)
C(6)	1448 (1)	3080 (1)	−1417 (2)	19 (1)
N(3)	5947 (1)	5126 (1)	947 (1)	16 (1)
O(1)	5558 (1)	5399 (2)	1933 (2)	31 (1)
O(2)	5652 (1)	5246 (1)	−220 (2)	22 (1)
O(3)	6610 (1)	4706 (1)	1112 (1)	23 (1)
O(*W*)	7950 (1)	5057 (1)	−1330 (2)	23 (1)

(II): Crystals of the Rh complex are colorless hexagonal prisms. Intensity data were collected at 120 (2) K using a spherical crystal 0.56 (2) mm in diameter. Range of indices, $-18 \le (h,k) \le 18$, $0 \le l \le 14$ ($4 < 2\theta \le 60°$); $0 \le (h,k) \le 28$, $0 \le l \le 21$ ($60 < 2\theta \le 100°$). There was no significant variation of five

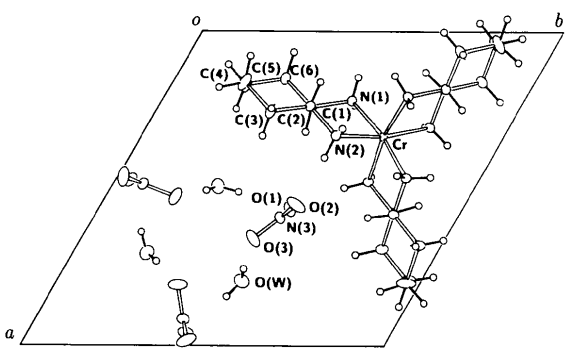

Fig. 1. Partial projection of the crystal structure of the Cr complex along the c axis.

Table 3. *Bond lengths* (Å) *and bond angles* (°)

	Cr	Rh
M—N(1)	2.092 (1)	2.084 (1)
M—N(2)	2.071 (1)	2.068 (1)
N(1)—C(1)	1.494 (2)	1.495 (3)
N(2)—C(2)	1.493 (1)	1.494 (2)
C(1)—C(2)	1.521 (1)	1.519 (3)
C(1)—C(6)	1.521 (2)	1.519 (2)
C(2)—C(3)	1.520 (2)	1.518 (4)
C(3)—C(4)	1.534 (2)	1.530 (3)
C(4)—C(5)	1.548 (4)	1.533 (5)
C(5)—C(6)	1.528 (3)	1.525 (4)
N(3)—O(1)	1.246 (2)	1.241 (3)
N(3)—O(2)	1.264 (2)	1.262 (2)
N(3)—O(3)	1.255 (2)	1.250 (2)
N(1)—*M*—N(2)	83.10 (5)	83.90 (5)
M—N(1)—C(1)	106.5 (1)	106.0 (1)
M—N(2)—C(2)	109.0 (1)	108.1 (1)
N(1)—C(1)—C(2)	106.5 (1)	106.7 (2)
N(1)—C(1)—C(6)	113.1 (1)	112.9 (2)
C(2)—C(1)—C(6)	111.6 (1)	111.7 (1)
N(2)—C(2)—C(1)	107.8 (1)	108.2 (1)
N(2)—C(2)—C(3)	112.5 (1)	112.5 (2)
C(1)—C(2)—C(3)	111.9 (1)	112.2 (2)
C(2)—C(3)—C(4)	110.8 (1)	111.1 (2)
C(3)—C(4)—C(5)	110.4 (1)	110.9 (2)
C(4)—C(5)—C(6)	109.8 (2)	110.6 (3)
C(1)—C(6)—C(5)	110.8 (1)	111.0 (2)
O(1)—N(3)—O(2)	120.2 (1)	120.1 (2)
O(1)—N(3)—O(3)	120.0 (1)	119.9 (2)
O(2)—N(3)—O(3)	119.8 (1)	120.0 (2)

standard reflections, $0.995 < |F_o|/|F_o|_{\text{initial}} < 1.005$. 13 235 reflections were measured, 12 061 reflections were observed with $|F_o| > 3\sigma(|F_o|)$, and 4602 unique reflections were obtained ($R_{\text{int}} = 0.011$). Absorption corrections with $\mu r = 0.177$ were made ($0.769 < A < 0.774$).

Refinement

At first, conventional refinement was attempted using the full-matrix least-squares program *MOLLY* (Hansen & Coppens, 1978) without multipoles (refinement *A*). As the extinction effect was negligible, subsequent refinements were carried out without an extinction correction. Scattering factors of core and valence shells of non-H atoms were taken from *International Tables for X-ray Crystallography* (1974, Vol. IV). For H atoms, scattering factors were those of Stewart, Davidson & Simpson (1965). The function $\sum w(|F_o| - |F_c|)^2$ was minimized with weights $w^{-1} = \sigma^2(|F_o|) + (0.015|F_o|)^2$. Refinement information is listed in Table 1. The structural chirality was assigned with reference to the known absolute configuration of the ligand, (−)-*R*,*R*-chxn (Miyamae, Sato & Saito, 1977). For the enantiomeric structures, the *R* values increased: $R = 0.051$ and $wR = 0.041$ for Cr, and $R = 0.032$ and $wR = 0.031$ for the Rh crystal.

In refinement *B*, multipoles were included up to the hexadecapole level for all non-H atoms. The radial functions are $r^{n_l}\exp(-\zeta r)$ with $n_l = 4$ for all l values (Cr, Rh) and $n_l = 2, 2, 2, 3, 4$ for $l = 0, 1, 2, 3, 4$ (O, N and C). The positional, thermal, multipole and ζ (shielding) parameters were refined. Initial ζ values were taken from Clementi & Raimondi (1963) for Cr, O, N and C atoms and that for Rh was obtained assuming the shielding-constants rule proposed by Slater (see Eyring, Walter & Kimball, 1944). The 4*s* and 4*p* orbital populations of Cr and the 5*s* and 5*p* orbital populations of Rh were not taken into account. Chemical symmetry 32 (D_3) of the complex cation was assumed. Symmetry constraints on the multipole parameters were imposed upon NO_3^- (D_{3h}) and H_2O (C_{2v}) in order to reduce the number of multipole parameters. The total charge of the unit cell was constrained to be neutral. For H atoms, no multipoles were introduced and the valence-electron populations were fixed at unity in order to avoid an unrealistic result. Partial projections of the crystal structures are presented in Fig. 1 together with the atom-numbering scheme. Atomic coordinates are listed in Table 2, and bond lengths and angles in Table 3.* Hydrogen-bond lengths involving the ligating N atoms are listed in Table 4.

Table 4. *Hydrogen-bond lengths* (Å) *involving the ligating* N *atoms*

	Cr	Rh
N(1)···O(2^{i})	3.123 (2)	3.116 (2)
N(1)···O(3^{ii})	3.102 (2)	3.127 (2)
N(2)···O(1)	2.990 (2)	2.987 (2)
N(2)···O(*W*^{iii})	2.887 (2)	2.891 (2)

Symmetry codes: (i) $-x+y, 1-x, z$; (ii) $1-x, 1-y, z-\frac{1}{2}$; (iii) $1-x, 1-y, z+\frac{1}{2}$.

Table 5. *Electron populations for the metal d orbitals*

	Cr	Co*	Rh
Total	3.42 (7)	5.98 (8)	7.12 (12)
a_1	0.95 (5)	1.71 (6)	1.90 (6)
e	1.87 (10)	3.12 (12)	3.83 (13)
e'	0.60 (10)	1.15 (12)	1.39 (13)
$e, e', + e_-e'$	0.55 (12)	0.23 (14)	0.40 (15)

* Morooka, Ohba, Saito & Miyamae (1991).

Electron populations of the Cr and Rh *d* orbitals are listed in Table 5 and were derived from the multipole coefficients (Holladay, Leung & Coppens, 1983). Equations giving the orbital populations as linear combinations of the multipole parameters are contained in the previous paper (Morooka, Ohba, Saito & Miyamae, 1991). Computations were carried out on a MIPS RS3230 Workstation.

* Lists of structure factors, anisotropic thermal parameters, positional parameters of H atoms, bond lengths and bond angles involving H atoms, and multipole parameters have been deposited with the British Library Document Supply Centre as Supplementary Publication No. SUP 55158 (31 pp.). Copies may be obtained through The Technical Editor, International Union of Crystallography, 5 Abbey Square, Chester CH1 2HU, England. [CIF reference: AS0599]

Discussion

Phase improvement

Deformation density maps around the Cr and Rh atoms after multipole refinement are shown in Fig. 2 and were calculated as the difference densities between the observed electron-density distribution and the superposition of those for spherical atoms with refined effective charges in order to show the charge asphericity around the metal atoms clearly. Deformation density maps calculated after conventional refinement are shown in Fig. 3. The negative troughs located perpendicular to the M—N bond in Fig. 3 disappeared after phase improvement (Fig. 2). This phenomenon was also found for the lel_3-Co^{III} complex (Morooka, Ohba, Saito & Miyamae, 1991). The deformation densities around the metal atoms mainly consist of the hexadecapole densities ρ_{40} and ρ_{43-}. The positive peaks on the threefold axis (z) correspond to ρ_{40} and the negative troughs on the M—N bond axes and positive peaks on the pseudo-threefold axes of the MN_6 octahedron correspond to both ρ_{40} and ρ_{43-}. From the phase errors based on the independent atom model (IAM), the features of ρ_{43-} are smeared and those of ρ_{40} remain [see Fig. 6

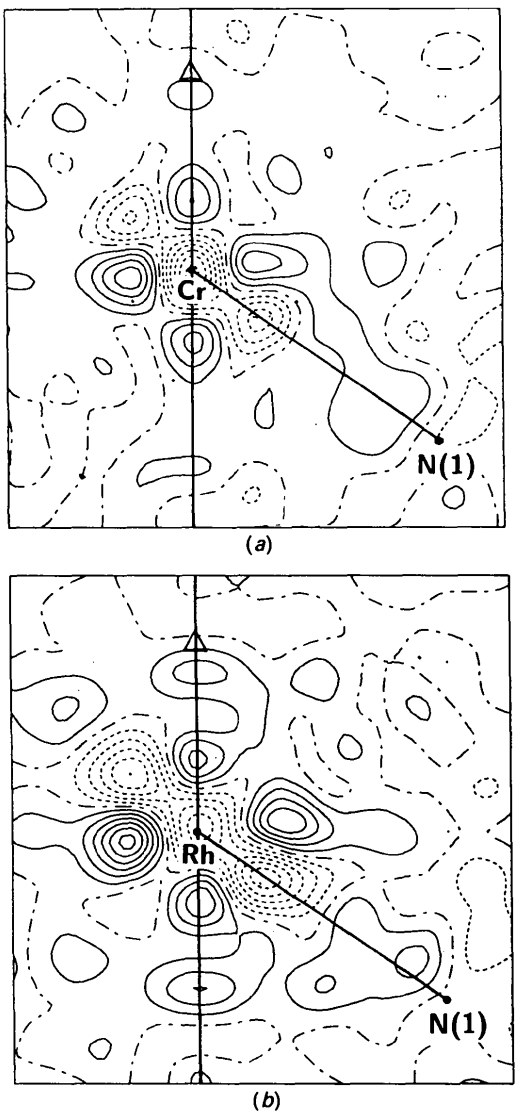

Fig. 2. Observed deformation density after phase improvement for (*a*) Cr and (*b*) Rh complexes. This is a section through an M—N bond and the threefold axis. Contour intervals at 0.2 e Å^{-3}. The standard deviations are (*a*) 0.09 and (*b*) 0.10 e Å^{-3} in the general position.

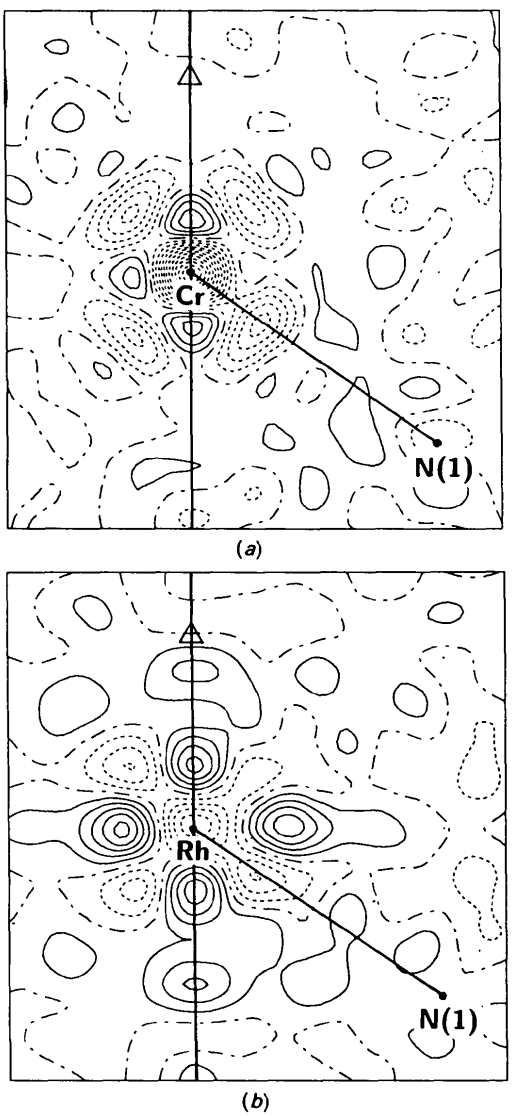

Fig. 3. Difference Fourier synthesis after conventional refinement (including phase error) for (*a*) Cr and (*b*) Rh complexes. The planes shown are the same as in Fig. 2. Contour intervals at 0.2 e Å^{-3}.

of Morooka, Ohba, Saito & Miyamae (1991)]. In order to understand this phenomenon, we consider F_{40} and F_{43-}, the contributions of ρ_{40} and ρ_{43-} to the structure factors. The phases of F_{40} and F_{43-} are limited to $n\pi/2$ depending on the parity of the reflection index l and on the parity of the multipole density to a rotation around z of 180°, as a result of the arrangement of the Co atoms in the unit cell [see Table 5 of Morooka, Ohba, Saito & Miyamae (1991)]. For the reflections to which the contribution of the metal atom is dominant, the phase of IAM is a good approximation to F_{00} (valence monopole) and F_{40}, but not explicitly for F_{43-}. For example, when l is even, F_{00} and F_{40} are real. On the other hand, F_{43-} is purely imaginary. This is the reason why the phase improvement for ρ_{43-} is still significant when the valence-/core-electron ratio becomes smaller for Cr^{III} and Rh^{III} complexes.

Charge asphericity

Dynamic multipole-model deformation density maps at the experimental resolution ($\sin\theta/\lambda \leq 1.08$ e Å^{-1}) are shown in Fig. 4, where the contributions of the unobserved reflections were supplemented. There are typical d-electron distributions in the approximately O_h ligand field. As seen from

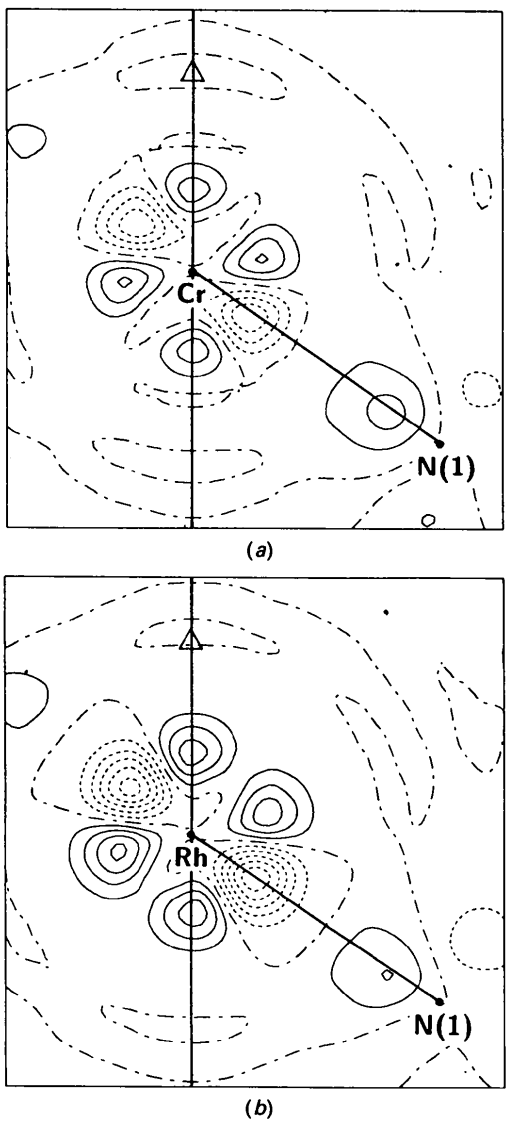

Fig. 4. Model deformation density based on all reflections within the range $\sin\theta/\lambda \leq 1.08$ Å^{-1} for (*a*) Cr complex with 5348 reflections and (*b*) Rh complex with 5382 reflections. The planes are the same as shown in Fig. 2. Contour intervals at 0.2 e Å^{-3}.

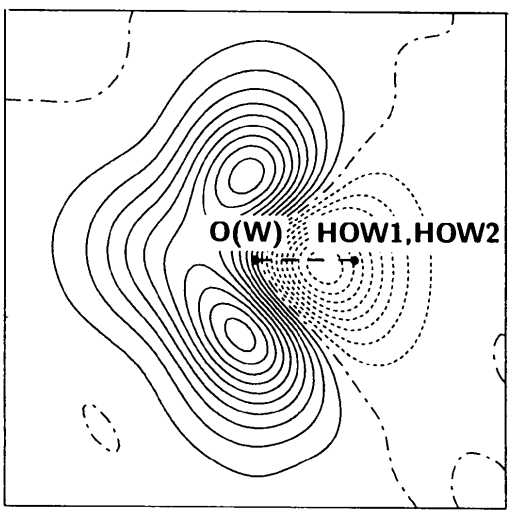

Fig. 5. Model deformation density in the plane bisecting the H—O—H bond angle and perpendicular to the H_2O molecule in the Cr crystal, $\sin\theta/\lambda \leq 1.08$ Å^{-1}. Contour intervals at 0.05 e Å^{-3}. The two hydrogen atoms HO*W*1 and HO*W*2 are shifted from the plane by ±0.64 Å.

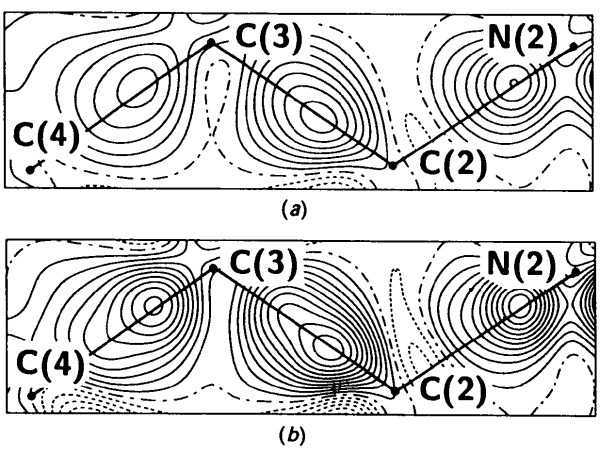

Fig. 6. (*a*) Dynamic and (*b*) static model deformation density in the plane containing the N(2)—C(2)—C(3) bond axes of the Cr complex, $\sin\theta/\lambda \leq 1.08$ Å^{-1}. Contour intervals at 0.05 e Å^{-3}.

Table 5, the ratios of the electron populations in the a_1 and e orbitals of the lel_3-$[M(chxn)_3]^{3+}$ (M = Cr, Co and Rh) complexes are 1:2 within experimental error. This accords with the fact that the coordination geometry around the metal atoms is nearly octahedral. The inclination angles of the M—N bond axes to the threefold axis are 54.57 (4)–54.98 (3), 54.23 (4)–54.55 (3) and 55.00 (4)–55.61 (3)° for lel_3-Cr, Co and Rh complexes, respectively. The corresponding angle for a regular octahedron is 54.74°. In the Co^{III} complex with the macrocyclic ligand hexaen (1,4,7,10,13,16-hexaazacyclooctadecane), the Co—N inclination angle is 59.312 (6)° and the population of the a_{1g} orbital is larger [by 9 (2)%] than that of the e_g orbitals, suggesting the lowest ligand field in the threefold axis (Morooka, Ohba & Toriumi, 1992). Comparing this result with the Co^{III} and Rh^{III} complexes, the asphericities in the 3*d*- and 4*d*-electron distributions seem to be essentially identical. A significant imbalance in the M—N bond lengths was observed for the series of $[M(chxn)_3](NO_3)_3.3H_2O$ crystals; however, it does not seem to be as a result of the hydrogen bonds (see Table 4).

The model deformation density map in the NO_3^- plane in the Cr crystal indicated the N—O bonding electrons and oxygen lone-pair electrons as was similarly observed in the Co crystal. The model deformation density in the plane bisecting the H—O—H bond angle is shown in Fig. 5. Lone-pair electrons of the O atom are observed as an elongated peak with double maxima. Fig. 6(*a*) is the model deformation density map of the chxn ligand in which the C—C and C—N bonding electrons are observed. The subtracted promolecule for Fig. 6 is the independent atom model with neutral atomic charges in order to compare the peak heights based on the same reference atomic densities. The density on the C(3)—C(4) axis is lower than that on the C(2)—C(3) axis because of the larger thermal vibration of the C(4) atom, which is further from the metal center than C(2). The peak heights on the C(2)—C(3) and C(3)—C(4) bonds are nearly equal in the static model map (Fig. 6*b*).

We are grateful to Dr Frode Galsbøl of the H. C. Ørsted Institute, University of Copenhagen, for supplying the crystals.

References

CLEMENTI, E. & RAIMONDI, D. L. (1963). *J. Chem. Phys.* **38**, 2686–2689.

EYRING, H., WALTER, J. & KIMBALL, G. E. (1944). *Quantum Chemistry*, pp. 161–163. New York: John Wiley.

GALSBØL, F. (1978). *Acta Chem. Scand. Ser. A*, **32**, 757–761.

GALSBØL, F., STEENBØL, P. & SØRENSEN, B. S. (1972). *Acta Chem. Scand.* **26**, 3605–3611.

HANSEN, N. K. & COPPENS, P. (1978). *Acta Cryst.* A**34**, 909–921.

HARNUNG, S. E. & LAIER, T. (1978). *Acta Chem. Scand. Ser. A*, **32**, 41–45.

HARNUNG, S. E., SØRENSEN, B. S., CREASER, I., MAEGAARD, H., PFENNINGER, U. & SCHÄFFER, C. E. (1976). *Inorg. Chem.* **15**, 2123–2126.

HIRSHFELD, F. L. (1971). *Acta Cryst.* B**27**, 769–781.

HOLLADAY, A., LEUNG, P. & COPPENS, P. (1983). *Acta Cryst.* A**39**, 377–387.

MIYAMAE, H. (1977). Thesis, Univ. of Tokyo, Japan.

MIYAMAE, H., SATO, S. & SAITO, Y. (1977). *Acta Cryst.* B**33**, 3391–3396.

MOROOKA, M., OHBA, S., SAITO, Y. & MIYAMAE, H. (1991). *Acta Cryst.* B**47**, 910–917.

MOROOKA, M., OHBA, S. & TORIUMI, T. (1992). *Acta Cryst.* B**48**, 459–463.

STEWART, R. F., DAVIDSON, E. R. & SIMPSON, W. T. (1965). *J. Chem. Phys.* **42**, 3175–3187.

Acta Cryst. (1992). B**48**, 672–677

Etude des Energies d'Interactions Moléculaires dans la Polymérisation à l'Etat Cristallin du Bis[(*p*-chlorophényl)carbamate] de Hexadiyne-2,4 Diyle-1,6 (1*p*CPU)

PAR PIERRE SPINAT ET CATHERINE BROUTY

Laboratoire de Minéralogie–Cristallographie des Universités Pierre et Marie Curie et Paris VII, *associé au CNRS* (*UA* 09), 4 *Place Jussieu, Tour* 16, 75252 *Paris CEDEX* 05, *France*

(*Reçu le* 23 *décembre* 1991, *accepté le* 17 *février* 1992)

Abstract

Conformational and van der Waals interactions have been studied during the solid-state homogeneous polymerization of the urethane diacetylene compound 1*p*CPU ($C_{20}H_{14}Cl_2N_2O_4$). Refinement was achieved by minimization of all intra- and intermolecular energies (hydrogen-bond energies included), for all monomer and polymer molecules. It is established that the free molecule and the molecule in the crystal adopt different conformations, the first being characterized by a lower energy state

0108-7681/92/050672-06$06.00